THE JOURNAL OF BIOLOGICAL CHEMISTRY VOL. 290, NO. 27, pp. 16478–16488, July 3, 2015

The Tyrosine Kinase c-Abl Promotes Homeodomain-interacting Protein Kinase 2 (HIPK2) Accumulation and Activation in Response to DNA Damage*◆

Received for publication, November 27, 2014, and in revised form, May 4, 2015 Published, JBC Papers in Press, May 5, 2015, DOI 10.1074/jbc.M114.628982

Nina Reuven[‡], Julia Adler[‡], Ziv Porat[§], Tilman Polonio-Vallon[¶], Thomas G. Hofmann[¶], and Yosef Shaul[‡1]

From the [‡]Department of Molecular Genetics and the [§]Biological Services Unit, Weizmann Institute of Science, Rehovot 76100, Israel and the [¶]Cellular Senescence Group, Cell and Tumor Biology Program, Deutsches Krebsforschungszentrum (DKFZ), DKFZ-ZMBH Alliance, 69120 Heidelberg, Germany

Background: c-Abl tyrosine kinase and serine/threonine kinase HIPK2 are activated by DNA damage and promote apoptosis.
Results: c-Abl phosphorylated HIPK2, and this enabled HIPK2 accumulation and phosphorylation of p53 in response to γ- and UV radiation.
Conclusion: HIPK2 response to DNA damage depends on c-Abl kinase activity.
Significance: This work demonstrates a new role for c-Abl in regulating p53 apoptotic response.

The non-receptor tyrosine kinase c-Abl is activated in response to DNA damage and induces p73-dependent apoptosis. Here, we investigated c-Abl regulation of the homeodomain-interacting protein kinase 2 (HIPK2), an important regulator of p53-dependent apoptosis. c-Abl phosphorylated HIPK2 at several sites, and phosphorylation by c-Abl protected HIPK2 from degradation mediated by the ubiquitin E3 ligase Siah-1. c-Abl and HIPK2 synergized in activating p53 on apoptotic promoters in a reporter assay, and c-Abl was required for endogenous HIPK2 accumulation and phosphorylation of p53 at Ser[46] in response to DNA damage by γ- and UV radiation. Accumulation of HIPK2 in nuclear speckles and association with promyelocytic leukemia protein (PML) in response to DNA damage were also dependent on c-Abl activity. At high cell density, the Hippo pathway inhibits DNA damage-induced c-Abl activation. Under this condition, DNA damage-induced HIPK2 accumulation, phosphorylation of p53 at Ser[46], and apoptosis were attenuated. These data demonstrate a new mechanism for the induction of DNA damage-induced apoptosis by c-Abl and illustrate network interactions between serine/threonine and tyrosine kinases that dictate cell fate.

The cellular DNA damage response comprises mechanisms to repair DNA, as well as pathways that lead to senescence or apoptosis, depending on the level of damage and internal and external cellular conditions. The p53 tumor suppressor is a central effector of the DNA damage response, and it is guided to trigger varied responses through its post-translational modifications. Phosphorylation of p53 at Ser[46] following DNA damage is associated with preferential induction of a pro-apoptotic program through specific association of phospho-Ser[46] p53 with promoters of pro-apoptotic genes (1, 2) as well as facilitating the p53 direct mitochondrial apoptotic program (3). Phosphorylation of p53 at Ser[46] also promotes the association of p53 with Pin1, which in turn mediates the dissociation of p53 from the inhibitor of apoptosis stimulating protein of p53 (iASPP) (4) and promotes Pin1-mediated activation of the mitochondrial death program of p53 (5).

Homeodomain-interacting protein kinase 2 (HIPK2)[2] is a serine/threonine kinase that primes p53-mediated apoptosis. In response to DNA damage by genotoxic agents such as ionizing and UV radiation, HIPK2 accumulates and phosphorylates p53 at Ser[46], thereby inducing apoptosis both by increasing transcription of pro-apoptotic genes and through an increase in the p53 direct mitochondrial apoptotic program (3, 5–9). Upon activation, HIPK2 autophosphorylates on serine/threonine as well as on tyrosine residues. Autophosphorylation at Ser[357] and Tyr[354] is necessary for HIPK2 kinase activity, binding to substrates and to Pin1 (10, 11). HIPK2 also autophosphorylates upon DNA damage at Thr[880]/Ser[882], and these modifications are involved in HIPK2 interaction with Pin1 (12). HIPK2 localization to PML nuclear bodies in the nucleus aids in its activation, escape from degradation mediated by E3 ubiquitin ligases, and activation of p53 (6, 13, 14). Phosphorylation of HIPK2 by Src causes HIPK2 to localize to the cytoplasm, preventing its activation of p53 (15). In unstressed cells, HIPK2 is maintained at a low level through ubiquitination and proteasomal degradation. Several E3 ubiquitin ligases, including Siah-1 and -2 (16, 17), WSB-1 (18), Mdm2 (19), and SCF(Fbx3) (14), are responsible for promoting this degradation, which is inhibited upon

* This work was supported by grants from the Israel Science Foundation (Grant 551/11), the Israel Cancer Research Fund, the Cooperation Program in Cancer Research of the Deutsches Krebsforschungszentrum (DKFZ) and Israel's Ministry of Science and Technology (MOST), and the Minerva Foundation with funding from the Federal German Ministry for Education and Research. This work was also supported by the SFB 1036 from the Deutsche Forschungsgemeinschaft (DFG) (to T. G. H.).
◆ This article was selected as a Paper of the Week.
[1] To whom correspondence should be addressed. Tel.: 972-8-9342320; Fax: 972-8-9344108; Email: yosef.shaul@weizmann.ac.il.

[2] The abbreviations used are: HIPK2, homeodomain-interacting protein kinase 2; PML, promyelocytic leukemia protein; ATM, ataxia telangiectasia-mutated; ATR, ATM and Rad3-related; IR, irradiation; IP, immunoprecipitation; Gy, grays.

genotoxic stress. Degradation of HIPK2 by Siah-1 is inhibited by phosphorylation of Siah-1 by ATM and ATR upon DNA damage (16). Interaction of HIPK2 with Pin1 or phosphorylation by Src also reduces HIPK2 interaction with Siah-1 and polyubiquitination (12, 15).

The non-receptor tyrosine kinase c-Abl is activated upon DNA damage and promotes apoptosis through the Yap-p73 pathway (20, 21). Phosphorylation of Yap by c-Abl causes Yap to preferentially associate with p73 at apoptotic gene targets, instead of cell cycle arrest targets (21), and to associate with p73 rather than with other transcription factors such as Runx (22). Thus, c-Abl supports the p73 pro-apoptotic DNA damage response. Targeted activation of the c-Abl/Yap-p73 pathway has recently been demonstrated to be a powerful mechanism for cancer cell killing (23). c-Abl also promotes p53-dependent DNA damage-induced apoptosis indirectly through modulation of upstream regulators such as Mdm2, ATM/ATR, and p38 MAPK (24–26). c-Abl activates p73 through direct phosphorylation (20, 27), but c-Abl does not directly phosphorylate p53 (28). HIPK2 possesses several consensus sites for c-Abl phosphorylation (Y*XX*P), suggesting a possibility of direct phosphorylation and regulation of HIPK2 by c-Abl.

Cellular environments influence DNA damage response. The Hippo pathway, activated by cell crowding, inhibits DNA damage-induced apoptosis mediated by c-Abl (29). This occurs through inhibition of c-Abl by the Hippo pathway kinase Lats2. Thus, Hippo inhibits apoptosis mediated by Yap/p73. However, high cell density also inhibits DNA damage-induced apoptosis in cells with wild-type p53. It was shown that cell crowding reduces p53 apoptotic activity in response to genotoxic stress (30). However, the mechanism for inhibition of p53-dependent apoptosis at high cell density remained unknown.

Our results show that c-Abl activity was required for the accumulation and activity of HIPK2 in response to γ- and UV radiation and synergized with HIPK2 in the activation of pro-apoptotic p53 target genes. c-Abl phosphorylated HIPK2 on several sites, and c-Abl prevented degradation of HIPK2 mediated by the ubiquitin E3 ligase Siah-1. Lats2 inhibited c-Abl phosphorylation of HIPK2, and HIPK2 accumulation and phosphorylation of p53 at Ser^{46} were inhibited at high cell density. These findings demonstrate a new link between the tyrosine kinase c-Abl and the serine/threonine kinase HIPK2 in promoting DNA damage-induced apoptosis and help to explain how apoptosis is inhibited at high cell density.

Experimental Procedures

Cells and Cell Culture—The cell lines used were human embryonic kidney cells HEK 293 and HEK 293T, HepG2, and Hep3B cells. Cells were grown in DMEM (DMEM; Gibco, Life Technologies, Thermo Scientific) supplemented with 8% fetal bovine serum (Gibco), 100 units/ml penicillin, 100 μg/ml streptomycin and cultured at 37 °C in a humidified incubator with 5.0% CO_2. Plating densities are defined as <40% confluent for "sparse" and confluent for "dense." Unless otherwise specified, cells were plated under sparse conditions. After plating, cells were allowed to attach for at least 16 h before treatment (such as irradiation) or harvesting. Light microscopy photographs of cells were performed using an Olympus (Tokyo, Japan) IX70 microscope connected to a DVC camera.

Plasmids, Transfection, Transduction, and mRNA Analysis—The plasmids used were: pCDNA3 c-Abl Δ1–81 and K290H (kinase-dead) (29). Full-length c-Abl constructs were the 1b isoform, and numbering of c-Abl residues refers to the positions in the 1b isoform. pSG5 c-Abl WT and ΔSH3 were described (20). The pSG5 c-Abl 1–730 and 1–1044 mutants were made by cleaving the wild-type clone with BamHI and either AfeI or EheI, respectively, and ligating along with a blunt-BamHI linker containing stop codons. Human pCDNA3 FLAG-HIPK2 full-length, K221A (kinase-dead), truncation, and GFP-fused constructs and HA-Siah-1 constructs have been previously described (16). mRFP-PML IV was described in Ref. 31. FLAG-HIPK2 constructs in the pCDNA3 vector backbone were also transferred to the pEFIRES vector (32). FLAG-HIPK2 constructs were also transferred to the pTriEx expression vector (Novagen, Merck Millipore), for bacterial expression of N-terminally His-tagged proteins. Site-directed mutagenesis, confirmed by sequencing, was used to create point mutations described in the text. Mdm2 (33), pRc/CMV p53, FLAG-p53, and Myc-Lats2 constructs (34) were provided by M. Oren and Y. Aylon. For stable knocking down of c-Abl, HEK 293T cells were transfected with the mission pLKO.1 shRNA vectors targeting c-Abl or GFP or harboring a non-targeting sequence (Sigma) together with pLP1, pLP2, and pLP-VSVG packaging plasmids (Invitrogen, Life Technologies, Thermo Scientific). 48 h hours after transfection, viral supernatant was filtered through a 0.45-μm filter, supplemented with 8 μg/ml Polybrene, and used to infect Hep3B or HepG2. 24 h after infection, cells were selected with 2 μg/ml puromycin (Sigma) or 5 μg/ml blasticidin (Calbiochem (Merck Millipore)) in the culture medium. To generate Hep3B cells stably expressing p53, retrovirus infection was performed by transfecting 293 Phoenix retrovirus packaging cells with p53 expression vector or the respective empty vector. Transduction of Hep3B with retrovirus particles was performed using the same protocol as described above for the lentiviral vectors. All transfections of HEK293 and HEK293T cells were done by the calcium phosphate method as described (35). JetPEI® (Polyplus Transfection SA, Illkirch, France) was used to transfect Hep3B cells. Total RNA was extracted using the TRI Reagent solution (Molecular Research Center, Cincinnati, OH), DNase-treated using the RNase-free DNase set (Qiagen, Hilden, Germany), and then reverse-transcribed by iScript cDNA synthesis kit (Bio-Rad). Quantitative RT-PCR was performed with SYBR® Green PCR master mix (Kapa Biosystems, Woburn, MA) using the LightCycler® 480 instrument (Roche Diagnostics, Basel, Switzerland).

GST Pulldown Assay—GST fusion proteins were expressed in the *Escherichia coli* BL21 strain and purified using GSH-Sepharose 4B beads (GE Healthcare). GST-HIPK2 (1–520) and GST-HIPK2 (551–1191) fusion proteins were incubated with ^{35}S-labeled c-Abl generated by *in vitro* translation using the TNT coupled reticulocyte lysate system (Promega) according to the manufacturer's instructions. In brief, reticulocyte lysates were incubated with bead-bound GST fusion proteins in AM200 buffer (20 mM Tris-HCl, pH 7.9, 200 mM KCl, 5 mM

$MgCl_2$, 0.1 mM EDTA, 0.5 mM EGTA, 10% glycerol, 0.05% Nonidet P-40) for 2 h at 4 °C. Afterward the beads were washed three times using AM200 buffer. Finally the proteins were eluted using 1× Laemmli buffer. GST pulldowns were analyzed by SDS-PAGE and autoradiography. 10% input was loaded as input control. Total amounts of proteins were analyzed by Coomassie Brilliant Blue staining.

In Vitro Kinase Assays—*In vitro* kinase assays were performed as described (29), with some modifications. HEK293 cells were transfected with c-Abl constructs. Proteins were immunoprecipitated using anti-c-Abl K12 (Santa Cruz Biotechnology) with protein A/G-Sepharose (Santa Cruz Biotechnology). Immunoprecipitates were washed four times with lysis buffer and then twice with kinase buffer (50 mM Tris-Cl, pH 7.5, 10 mM $MgCl_2$, 1 mM EGTA, 2 mM DTT, and 0.01% Brij 35). For the assay, bacterially expressed and purified recombinant proteins or control were added to the tubes containing the immunoprecipitated c-Abl (not eluted from the beads). BSA was added to 200 μg/ml, and ATP was added to 200 μM. Reactions were incubated at 30 °C for 30 min. The reactions were centrifuged, and the supernatant (assay mix) and pellets (containing c-Abl) were analyzed separately by SDS-PAGE and immunoblotting.

Immunoblot and Coimmunoprecipitation Studies—Immunoblots and immunoprecipitations (IPs) were done as described previously (35). Affinity-purified rabbit polyclonal anti-HIPK2 antibodies, (batches 88a, C1, and rb1) were previously described (16). All batches were raised against the same peptide antigen, and all batches detected endogenous HIPK2. There were some differences in cross-reacting bands among the different batches. Other antibodies used were: anti-HA, monoclonal anti-β-tubulin, anti-β-actin, and anti-FLAG M5 (Sigma); anti-c-Abl K12, anti-c-Abl 8E9, and anti-general phosphotyrosine (phospho-Tyr (PY20), Santa Cruz Biotechnology, Santa Cruz, CA); anti-cleaved caspase-3, anti-phospho-Ser^{46} p53 (Cell Signaling, Beverly, MA). The anti-c-Abl K12 antibody was used for c-Abl detection, unless otherwise specified. Monoclonal anti-p53 DO-1 antibodies were a generous gift from C. Prives. Anti-Myc monoclonal antibodies were generated by the Antibody Laboratory of the Weizmann Institute. For IP of HA- and FLAG-tagged proteins, anti-FLAG M2-agarose and anti-HA-agarose (Sigma) were used. For other IPs, protein A/G-agarose (Santa Cruz Biotechnology) was used. Horseradish peroxidase-conjugated secondary antibodies were from Jackson ImmunoResearch Laboratories, West Grove, PA. Enhanced chemiluminescence was performed with the EZ-ECL kit (Biological Industries, Kibbutz Beit Haemek, Israel), and signals were detected by the ImageQuant LAS 4000 (GE Healthcare) or by exposure to film. Intensities of bands were quantified by the ImageQuant TL software. For comparison of multiple experiments, values within one experiment were normalized to a standard set at 1. Error bars represent S.E.

Immunofluorescence Staining—Cells were seeded on glass coverslips and UV-irradiated the next day, and 24 h following irradiation, cells were fixed in 4% paraformaldehyde for 30 min, permeabilized with 0.5% (v/v) Triton-X-100 for 25 min, and blocked with 10% BSA and 0.2% Tween 20. Cells were incubated with either rabbit polyclonal anti-phospho-p53 (Ser^{46}) antibody (Cell Signaling) or rabbit polyclonal anti-c-Abl antibody (Santa Cruz) and mouse monoclonal anti-p53 hybridoma medium (DO-1) followed by the Alexa Fluor 488-conjugated donkey anti-rabbit or Alexa Fluor 555-conjugated donkey anti-mouse antibodies (Molecular probes). Slides were mounted with DAPI-containing Fluoromount-G (SouthernBiotech). Images were acquired using Zeiss LSM 710 confocal scanning system using a 60×/1.4 NA oil objective and processed by Zen 2009 software (Zeiss).

γ-Ray and UV Irradiation—Cells were subjected to γ-irradiation in a Millennium 870LC irradiator with a ^{137}Cs source (Mainance International Ltd., Waterlooville, Hampshire, UK). Cells were subjected to UV-C irradiation using a Stratagene UV Stratalinker 1800 (La Jolla, CA).

Reporter Gene Assays—HEK293 cells were transfected with plasmids expressing the tested constructs along with a promoter-containing firefly luciferase reporter plasmid, and a *Renilla* luciferase-expressing plasmid as a transfection control. 24 h after transfection, cell lysates were analyzed for luciferase activity in the Modulus microplate multimode reader (Turner Biosystems), and differences in transfection efficiency were corrected for by normalizing the firefly luciferase activity to that of *Renilla* luciferase.

Imaging Flow Cytometry—HEK293T cells were transfected with GFP-HIPK2 and H2B-RFP or mRFP-PML IV. 24 h after transfection, cells were treated with STI571 (20 μM) for 2 h and then subjected to UV irradiation (50J/m^2). 3 days after irradiation, cells were trypsinized, washed with PBS and run on the ImageStream X flow cytometer (Amnis Corp., Seattle, WA). Data were acquired using the INSPIRE software (Amnis Corp). At least 1000 GFP^+ and RFP^+ cells were imaged. To have an entire cell in optimal focus, the extended depth of field option was used (36). Data were deconvolved and analyzed by the IDEAS 6.0 software (Amnis Corp.). Cells were gated for single cells using the area and aspect ratio of the brightfield image and gated for focused cells using the gradient RMS feature (36). Nuclear mask was created according to H2B-RFP or staining with DRAQ5, which is confined to the nucleus. The number of individual spots within the nuclear mask was measured by using the Spot Count feature on the "Peak" mask.

Results

c-Abl Phosphorylates HIPK2—There are five putative consensus c-Abl phosphorylation sites (Y*XX*P) in HIPK2, two in the kinase domain, and three at the C terminus (Fig. 1*A*). In addition, HIPK2 autophosphorylates at Tyr^{354} (10, 11). To determine whether c-Abl has a role in phosphorylation of HIPK2 in response to DNA damage, we analyzed phosphorylation of HIPK2 in the presence or absence of the c-Abl inhibitor STI571 (Gleevec, imatinib). Our results indicated that irradiation increased the tyrosine phosphorylation of the endogenous HIPK2, and this was reduced with inhibition of c-Abl (Fig. 1*B*). To determine whether c-Abl could directly phosphorylate HIPK2, low levels of pCDNA3 FLAG-HIPK2 wild type and kinase-dead (K221A) were expressed with constitutively active c-Abl (c-Abl Δ1–81) (Fig. 1*C*). c-Abl phosphorylated both wild-type and kinase-dead HIPK2. In addition, c-Abl led to a dramatic increase in the accumulation of wild-type HIPK2,

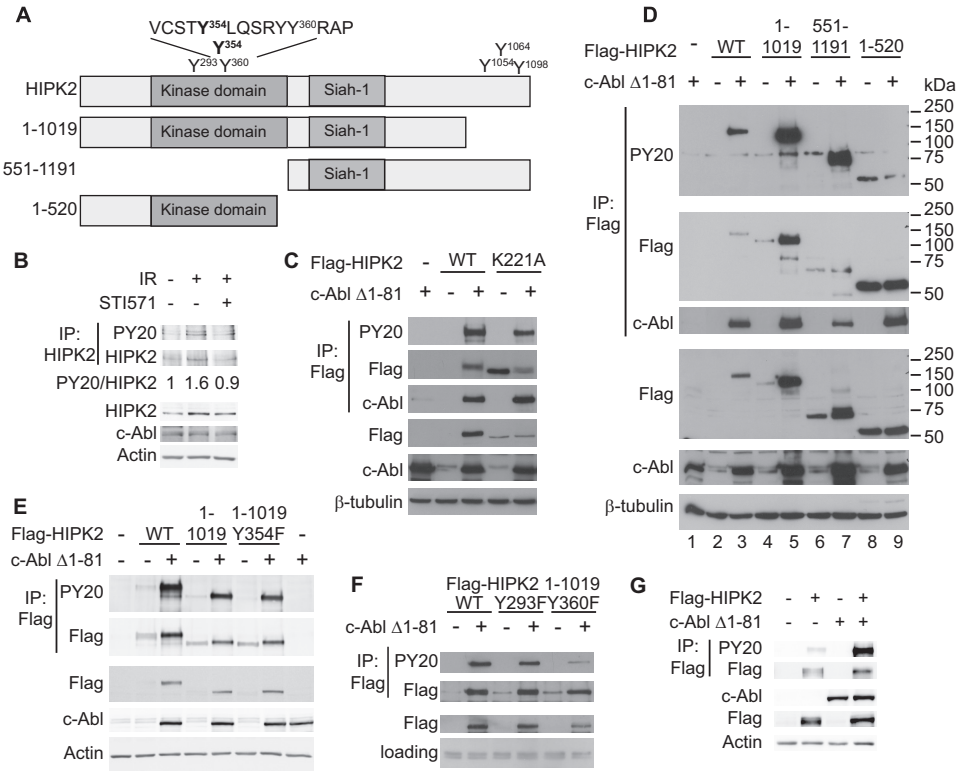

FIGURE 1. **c-Abl phosphorylates HIPK2 at several sites.** *A*, schematic representation of HIPK2 and truncation mutants. HIPK2 autophosphorylation site is indicated in *bold*. Sequence in the region of amino acids 350–363 is shown. The five putative c-Abl consensus phosphorylation sites are indicated, as well as HIPK2 kinase domain and Siah-1 interaction domain. All constructs have a FLAG tag at the N terminus. *B*, Hep3B cells were treated with 10 μM STI571 1 h prior to IR at 20 Gy. Cells were harvested 2 days after IR, and anti-HIPK2 was used for immunoprecipitation. Immunoprecipitated and total samples were analyzed by SDS-PAGE and immunoblotting. Phospho-Tyr (*PY20*) detects phosphotyrosine. The anti-HIPK2 C1 antibody was used for IP, and anti-HIPK2 rb1 was used for immunoblot detection. *C*, HEK293 cells were transfected with pCDNA3 FLAG-HIPK2 wild type and K221A and with constitutively active c-Abl Δ1–81 or with pCDNA3 empty vector, as indicated. Cells were harvested 24 h after transfection, and anti-FLAG was used for immunoprecipitation. Cells were analyzed as in *B*. *D*, HEK293 cells were transfected with pCDNA3 FLAG-HIPK2 wild type and truncation mutants and with c-Abl Δ1–81, as indicated. Cells were analyzed as in *B*. *E*, HEK293 cells were transfected with pCDNA3 FLAG-HIPK2 wild type, 1–1019 and 1–1019 Y354F mutants, and c-Abl Δ1–81, as indicated. Cells were analyzed as in *B*. *F*, HEK293 cells were transfected with pCDNA3 FLAG-HIPK2 1–1019 wild type and point mutants and with active c-Abl, as indicated. Cells were analyzed as in *B*. *G*, HEK293 cells were transfected with pEFIRES FLAG-HIPK2 and active c-Abl constructs, as indicated, and cells were analyzed as in *B*.

which was barely detectable under these conditions in the absence of c-Abl. The basal level of kinase-dead HIPK2 was higher than the wild type, and expression of c-Abl did not dramatically affect its accumulation. Nevertheless, this mutant was also tyrosine-phosphorylated in the presence of c-Abl. As noted above, HIPK2 autophosphorylates at Tyr^{354}; however, the kinase-dead mutant does not display this activity. Thus, the phosphorylation of the kinase-dead mutant, and by implication also of wild-type HIPK2, is likely mediated by c-Abl in *trans*, and not due to HIPK2 autophosphorylation. Furthermore, c-Abl co-immunoprecipitated with wild-type and kinase-dead HIPK2, implying a direct interaction (Fig. 1*C*).

To identify the putative c-Abl phosphorylation sites, we used truncation mutants of HIPK2. This analysis indicated that active c-Abl phosphorylated sites in both the N-terminal and the C-terminal halves of HIPK2 (Fig. 1*D*). To characterize the putative phosphorylation sites in the kinase domain, we used the HIPK2 truncation mutant 1–1019, which is missing the three putative C-terminal sites. c-Abl phosphorylated the C-terminally truncated HIPK2 with a mutation at the autophosphorylation site (Y354F) to the same degree as the wild-type control, indicating that the tyrosine phosphorylation was not due to activation of HIPK2 intrinsic autophosphorylation (Fig. 1*E*). Mutation of the c-Abl consensus phosphorylation sites in the kinase domain, Tyr^{293} and Tyr^{360}, showed that the Y360F mutant was poorly phosphorylated by c-Abl, indicating that Tyr^{360} appears to be a site of c-Abl phosphorylation (Fig. 1*F*). Interestingly, the Y360F mutant was also less stabilized by c-Abl, as indicated by the level of HIPK2 in the total cell extracts (Fig. 1*F*). These results suggest that c-Abl phosphorylation leads to the accumulation of HIPK2, at least in part via Tyr^{360} phosphorylation. As noted above (Fig. 1*C*), protein levels of full-length FLAG-HIPK2 expressed from the pCDNA3 vector were barely detectable by immunoblot, unless very high amounts of the vector were used. To increase HIPK2 levels, we also used the pEFIRES vector, which gave higher expression than pCDNA3. Using pEFIRES, high levels of FLAG-HIPK2 were observed even in the absence of c-Abl. Basal autophosphorylation of HIPK2 was seen under these conditions, but active c-Abl led to a large increase in HIPK2 phosphorylation (Fig. 1*G*), indicating that the phosphorylation observed with c-Abl expression was not merely due to the protein level of HIPK2.

Interaction of HIPK2 and c-Abl—To further explore the interaction between HIPK2 and c-Abl, we used truncation mutants of c-Abl (Fig. 2*A*). Here, the wild-type c-Abl construct used was full-length c-Abl, rather than the constitutively active Δ1–81 c-Abl mutant. All of the c-Abl constructs phosphorylat-

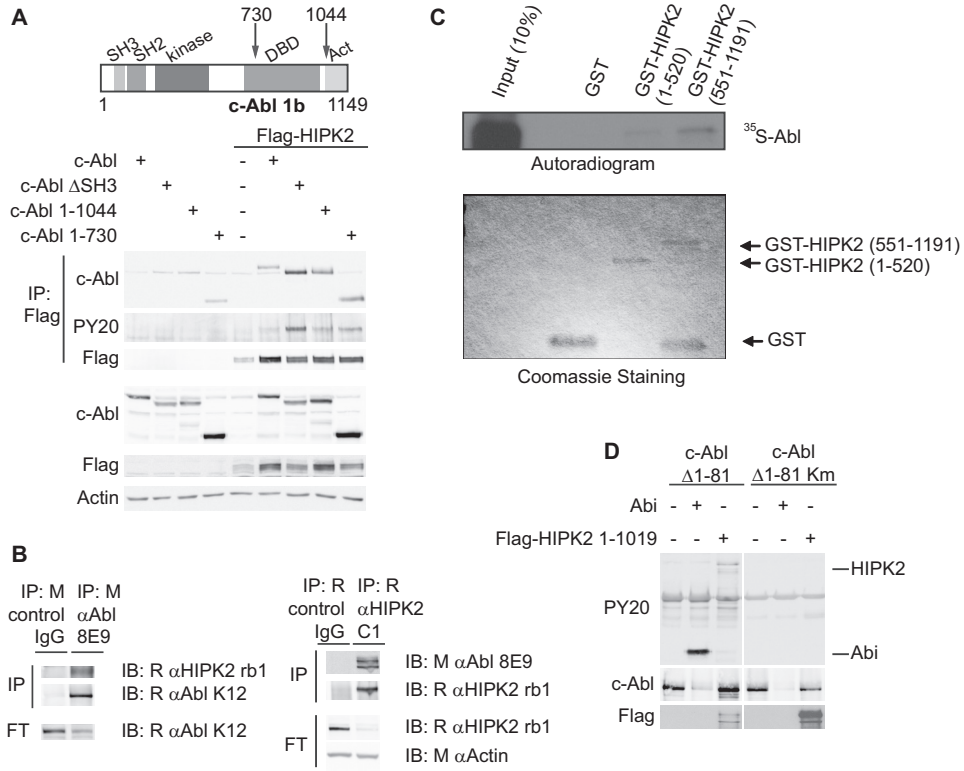

FIGURE 2. **Interaction between HIPK2 and c-Abl.** *A*, a schematic representation of c-Abl 1b is shown with the SH3, SH2, kinase, DNA binding (*DBD*), and G- and F-actin (*Act*) binding domains indicated. HEK293 cells were transfected with pEFIRES FLAG-HIPK2 and with pSG5 c-Abl wild type or truncation mutants, as indicated. Cells were harvested 24 h after transfection, and anti-FLAG was used for IP. Immunoprecipitates and total extracts were analyzed by SDS-PAGE and immunoblotting. *B*, a cell extract of HEK293 cells was divided into four samples and immunoprecipitated using rabbit anti-HIPK2 C1, control rabbit IgG, mouse anti-c-Abl 8E9, or control mouse IgG. Immunoprecipitated and immunodepleted "flow-through" (*FT*) samples were analyzed by SDS-PAGE and immunoblotting with the indicated antibodies. *R*, rabbit; *M*, mouse. *C*, *in vitro* interaction between HIPK2 truncations and c-Abl. GST-Hipk2 (1–520), GST-Hipk2 (551–1191), and GST were incubated with *in vitro* translated ^{35}S-labeled c-Abl. GST pulldowns were performed and analyzed by SDS-PAGE and autoradiography. 10% input was loaded as input control. Total amounts of proteins were analyzed by Coomassie Brilliant Blue staining. *D*, HEK293 cells were transfected with pCDNA3 c-Abl Δ1–81 wild type or kinase mutant (*Km*). The c-Abl constructs were immunoprecipitated and used in an *in vitro* assay (described under "Experimental Procedures") to phosphorylate bacterially expressed recombinant FLAG-HIPK2 1–1019 or a fragment of the control c-Abl substrate Abi. Following incubation for 30 min at 30 °C, the reactions were centrifuged, and the assay supernatant and the pellet fraction (containing Abl) were analyzed separately by SDS-PAGE and immunoblotting. The assay blot was probed first with the phospho-Tyr (*PY20*) antibody to detect phosphotyrosine and then stripped and probed with anti-FLAG.

ed and co-immunoprecipitated with HIPK2. Interestingly, even the ΔSH3 c-Abl mutant, missing the domain for interaction with P*XX*P motifs, interacted with HIPK2. Deletion of the extreme C terminus of c-Abl (1–1044 mutant), which comprises domains for binding to G- and F-actin, did not impair binding to HIPK2. On the other hand, the 1–730 mutant, although still capable of interacting with HIPK2, was less competent, considering the high expression level of this mutant. This suggests that the 730–1044 region of c-Abl contributes to the interaction between HIPK2 and c-Abl.

The overexpression experiments suggested a direct interaction between HIPK2 and c-Abl. To demonstrate that the endogenous proteins interact *in vivo*, we used reciprocal co-IP. Fig. 2*B* shows that endogenous c-Abl co-immunoprecipitated with endogenous HIPK2, and vice versa. To further show that the interaction between HIPK2 and c-Abl is direct, bacterially expressed recombinant fragments of HIPK2 were incubated with *in vitro* expressed and labeled c-Abl (Fig. 2*C*). Both the 1–520 and the 551–1191 recombinant fragments of HIPK2 interacted with c-Abl, with a slightly stronger association observed for the C-terminal fragment. These results demonstrate a direct interaction, mediated by domains found in both the N terminus and the C terminus of HIPK2.

To address the question of whether c-Abl could directly phosphorylate HIPK2, we employed an *in vitro* assay using bacterially expressed recombinant HIPK2. c-Abl Δ1–81 wild type or kinase mutant (K290H) was overexpressed in HEK293 cells and isolated by immunoprecipitation. Recombinant HIPK2 was phosphorylated *in vitro* by the immunoprecipitated wild-type, but not kinase-dead, c-Abl (Fig. 2*D*). Wild-type c-Abl also phosphorylated the recombinant fragment of Abi, which served as a positive control. Strong binding of Abi to Abl may have interfered with detection of Abl in these lanes. In addition, incomplete stripping of the phospho-Tyr (PY20) antibody from FLAG-HIPK2 is likely to have interfered with subsequent detection by the anti-FLAG antibody. These results show that c-Abl directly interacts with and phosphorylates HIPK2.

c-Abl Increases HIPK2 Activation of p53 Apoptotic Targets—We next determined whether phosphorylation of HIPK2 by c-Abl affected its activity. HIPK2 phosphorylates p53 at Ser^{46}, and the phosphorylation of p53 at Ser^{46} increases its activation of pro-apoptotic gene targets. To assess the role of c-Abl in inducing apoptotic genes through p53 and HIPK2, we used a luciferase reporter assay (Fig. 3). For this assay, we expressed HIPK2 using the pEFIRES vector, which gives high expression of HIPK2, and under the conditions used, the protein level of

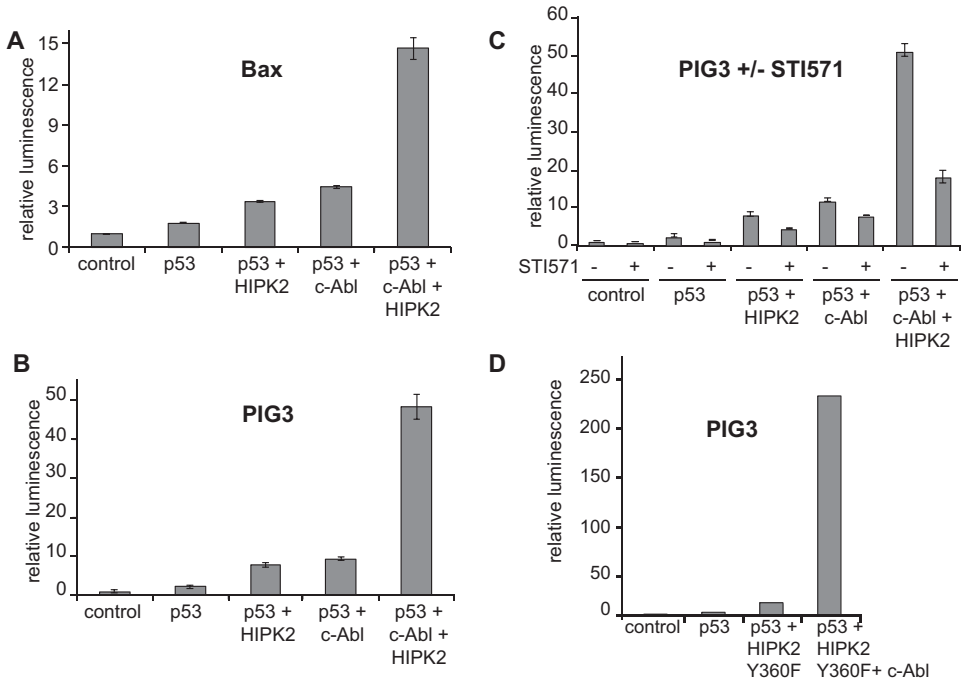

FIGURE 3. **c-Abl increases HIPK2 activation of p53 apoptotic targets.** *A–D*, HEK293 cells were transfected with p53, Bax luciferase, or PIG3 luciferase reporter plasmids, control *Renilla* luciferase plasmid, c-Abl Δ1–81, and pEFIRES FLAG-HIPK2 wild type (*A–C*) or Y360F (*D*). Cell extracts were prepared 24 h later and subjected to determination of luciferase and *Renilla* activity. Duplicate transfections were performed for analysis of protein levels. Reporter assay results are represented as -fold induction of luciferase activity normalized by *Renilla* activity, as compared with the control cells transfected with an empty expression vector. S.E. is calculated from at least three independent experiments. *A*, results using Bax reporter; *B* and *D*, results using PIG3 reporter; *C*, results using PIG3 reporter, in the presence or absence of 20 μM STI571 c-Abl inhibitor.

HIPK2 was not greatly affected by c-Abl (as seen in Fig. 1*G*). Expression of p53 alone led to slight induction of the target genes *Bax* and *PIG3*. When co-expressed with either c-Abl or HIPK2, induction of the target genes by p53 was moderately increased. However, when both HIPK2 and c-Abl were expressed with p53, the induction increased dramatically (Fig. 3, *A* and *B*). Treatment of the cells with the c-Abl inhibitor STI571 demonstrated that the effect required c-Abl kinase activity (Fig. 3*C*). We next tested the ability of the Y360F mutant to activate p53. Using the pEFIRES vector, this mutant, like the wild type, was expressed at high levels (data not shown). Previous studies had shown that this mutation does not impair HIPK2 kinase activity (10), and consistent with this observation, the Y360F mutant was active in inducing the p53 reporter (Fig. 3*D*). In addition, like the wild type, the effect was multiplied in the presence of c-Abl. These results indicate that c-Abl synergizes with HIPK2 in the induction of pro-apoptotic target genes by p53.

c-Abl Inhibits Degradation of HIPK2—Our results (Fig. 1) indicated that expression of active c-Abl led to an accumulation of HIPK2. To determine whether c-Abl could be affecting the protein stability of HIPK2, we compared the half-life of FLAG-HIPK2 in the presence or absence of active c-Abl. The level of FLAG-HIPK2 decreased over 12 h in the presence of cycloheximide, but with co-expression of c-Abl, FLAG-HIPK2 was stabilized (Fig. 4*A*). Our results above (Fig. 1*F*) had suggested that the FLAG-HIPK2 1–1019 Y360F mutant was less stable than the wild type. HIPK2 is a target of several E3 ligases, including Siah. To determine the role of c-Abl phosphorylation, as well as the Tyr^{360} residue, in the protection of HIPK2 from Siah-mediated degradation, we compared the ability of c-Abl to protect wild-type or Y360F full-length FLAG-HIPK2 from degradation by Siah-1 in transfected HEK293 cells (Fig. 4*B*). The level of wild-type FLAG-HIPK2 was reduced with co-expression of Siah-1. Constitutively active c-Abl, but not kinase-dead c-Abl, was able to mitigate Siah-1-mediated degradation. In contrast, the Y360F mutant was degraded with Siah-1 co-expression, and expression of c-Abl was not able to restore the level of HIPK2 (Fig. 4*B*).

HIPK2 Accumulation in Response to DNA Damage Requires an Active c-Abl—In response to DNA damage, HIPK2 protein accumulates. We next tested whether c-Abl is needed for accumulation of endogenous HIPK2 in response to DNA damage. Upon DNA damage by UV or γ-irradiation (IR), endogenous HIPK2 protein accumulated, but this was reduced in cells treated with the c-Abl inhibitor STI571 (Fig. 5, *A* and *B*). The effect was similar in p53-null Hep3B cells (Fig. 5*A*) as well as in p53-positive HEK293 cells (Fig. 5*B*), indicating that the effect is neither cell line-specific nor dependent on p53. The effect of c-Abl was on HIPK2 protein level, as RNA levels were not affected (Fig. 5*C*). STI571 inhibits ABL kinases, but also has been shown to inhibit a limited number of other kinases such as c-Kit and PDGF receptor (PDGFR) (37). To validate that HIPK2 accumulation in response to DNA damage depended on c-Abl, and was not a nonspecific effect of STI571, we used shRNA knockdown of c-Abl. Knockdown of c-Abl abrogated endogenous HIPK2 accumulation in response to DNA damage (Fig. 5*D*). Our results demonstrate that c-Abl is needed for endogenous HIPK2 response to both γ-radiation and UV radiation.

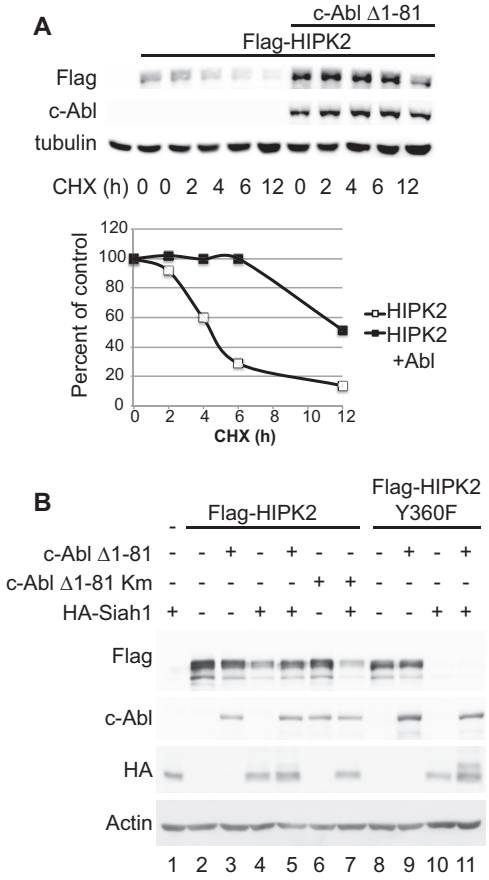

FIGURE 4. **c-Abl inhibits degradation of HIPK2.** *A*, HEK293 cells were transfected with pEFIRES FLAG-HIPK2 and c-Abl Δ1–81, as indicated. Cycloheximide (*CHX*) (500 μM) was added 24 h after transfection, and cells were harvested at the times indicated. Cells were analyzed by SDS-PAGE and immunoblotting. Quantification of the HIPK2 signal relative to tubulin is plotted in the graph below. *B*, HEK293T cells were transfected with pEFIRES FLAG-HIPK2 WT and Y360F (full-length clones), HA-Siah-1, and c-Abl Δ1–81 WT or kinase-mutant (*Km*), as indicated. Cells were harvested 25 h after transfection and were analyzed by SDS-PAGE and immunoblotting with the indicated antibodies.

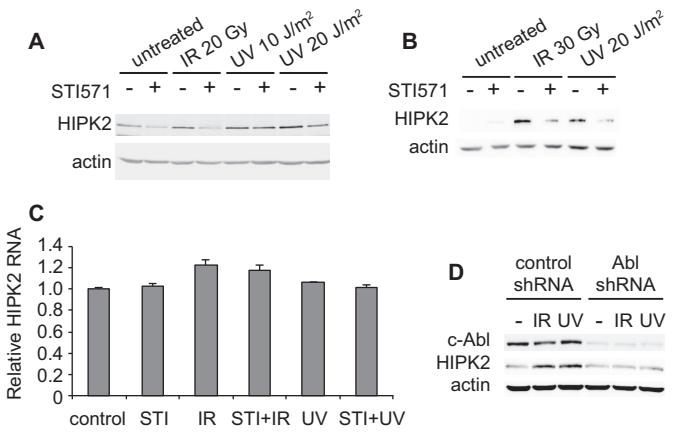

FIGURE 5. **c-Abl is needed for accumulation of HIPK2 in response to DNA damage.** *A*, Hep3B cells were treated with 20 μM STI571 (c-Abl inhibitor) or vehicle, as indicated, and exposed to 20 Gy of IR (γ-irradiation) or 10 or 20 J/m^2 UV, as indicated. Cells were harvested 24 h after irradiation and then analyzed by SDS-PAGE and immunoblotting with the indicated antibodies. Anti-HIPK2 88a was used to detect HIPK2. *B*, HEK293 cells were treated as in *A* and were exposed to 20 J/m^2 UV or 30 Gy of IR, as indicated, in duplicate. Cells were analyzed as in *A*. *C*, duplicate samples from *B* were analyzed for RNA. RNA was assayed by quantitative PCR and normalized by TBP1 mRNA levels. *STI*, STI571. S.E. is calculated from at least three independent experiments. *D*, Hep3B cells stably expressing shRNA to c-Abl or control were γ-irradiated (20 Gy) or UV-irradiated (20 J/m^2) and harvested 24 h later. Cells were analyzed as in *A*.

HIPK2 accumulates in nuclear speckles, which partially overlap with PML nuclear bodies, in response to DNA damage (6). Using a GFP-HIPK2 fusion construct, we analyzed the cells using ImageStream, a technique that combines FACS with single-cell microscopy for the analysis and quantification of fluorescent signals for hundreds of cells per sample. Using the Spot Count feature, we quantified the nuclear GFP-HIPK2 accumulation in speckles (Fig. 6*A*). This accumulation increased with UV and was reduced with inhibition of c-Abl. We also used ImageStream to quantify co-localization of GFP-HIPK2 with mRFP-PML IV in response to DNA damage. This analysis showed an increased association of HIPK2 with PML in response to UV irradiation. Interestingly, this association was reduced with inhibition of c-Abl (Fig. 6*B*). These results suggest that HIPK2 colocalization with PML in nuclear speckles in response to DNA damage depends on c-Abl activity.

HIPK2 Phosphorylation of p53 at Ser^{46} and Apoptotic Response to DNA Damage Are c-Abl-dependent—HIPK2 phosphorylates p53 on Ser^{46} in response to DNA damage. As was seen with the DNA damage-induced accumulation of HIPK2, the induction of phosphorylation of p53 at Ser^{46} was also inhibited by STI571 (Fig. 7*A*). This was observed in HepG2 cells that express endogenous p53. Furthermore, apoptosis, as seen by cleavage of caspase 3, was inhibited with c-Abl inhibition (Fig. 7*A*). In addition, a similar effect was observed in p53-null Hep3B cells upon reintroduction of p53 via transfection (Fig. 7*B*) or through stable transduction (Fig. 7*C*). Inhibition of c-Abl reduced p53 Ser^{46} phosphorylation that was induced by both IR (Fig. 7, *A* and *B*) and UV (Fig. 7*C*). Furthermore, DNA damage-induced expression of p53 target genes was blunted upon inhibition of c-Abl (Fig. 7*D*). Together these results demonstrate that c-Abl activity is needed for HIPK2 phosphorylation of p53 at Ser^{46} and the ensuing apoptotic response to DNA damage by IR and UV.

HIPK2 Accumulation and Activity Are Inhibited at High Cell Density—DNA damage-induced apoptosis is inhibited at high cell density, and we have recently demonstrated that the Hippo pathway, activated at high cell density, is involved in mediating this effect. The Hippo pathway kinase Lats2 inhibits c-Abl activity and prevents the phosphorylation of the downstream substrates Yap and p73 (29). Because our data showed that c-Abl was needed for accumulation and activation of HIPK2 in response to DNA damage, we wanted to know whether high cell density, as well as Lats2, would likewise inhibit HIPK2. As predicted, overexpression of Lats2 reduced the phosphorylation and accumulation of HIPK2 by active c-Abl (Fig. 8*A*). High cell density inhibits c-Abl activation in response to DNA damage (29). To determine whether HIPK2 accumulation is inhibited under this condition, Hep3B cells were plated under sparse and dense conditions and treated with IR or UV. High cell density prevented HIPK2 accumulation in response to both IR and UV (Fig. 8*B*). Furthermore, phosphorylation of p53 at Ser^{46} and induction of apoptosis, as seen by cleavage of caspase 3, were reduced in densely plated cells (Fig. 8, *C* and *D*). Taken together,

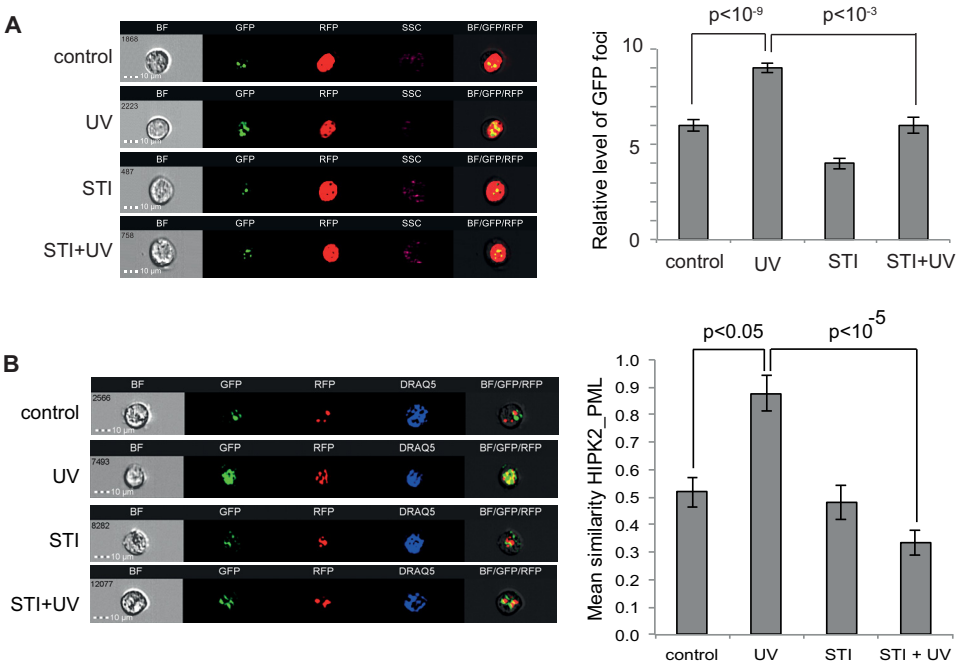

FIGURE 6. **Accumulation of HIPK2 in nuclear speckles is dependent on c-Abl.** *A*, HEK293T cells were transfected with plasmids expressing GFP-HIPK2 and RFP-histone H2B. Cells were treated with 20 μM STI571 (*STI*) or vehicle, as indicated, and irradiated at 50 J/m^2 (UV). Cells were analyzed using the ImageStream X flow cytometer 72 h after irradiation. The *left panels* show bright field (*BF*) images, GFP-HIPK2, RFP-H2B (nuclear marker), side scatter, and merged images (*BF/GFP/RFP*) of representative control and UV-treated cells, with or without the c-Abl inhibitor STI571. The *right panel* shows quantification of GFP-HIPK2 spot count in the differently treated cell populations. Data represent S.E. from three independent experiments. The Student's *t* test was used to evaluate statistical significance. *B*, HEK293 cells were transfected with plasmids expressing GFP-HIPK2 and mRFP-PML IV. Cells were treated with 12.5 μM STI571 or vehicle, as indicated, and irradiated at 50 J/m^2. Cells were analyzed as in *A*, but DRAQ5 staining was used to define the nucleus. The *left panels* show bright field (*BF*) images, GFP-HIPK2, RFP-PML IV, DRAQ5 (nuclear staining), and merged images (*BF/GFP/RFP*) of representative control and UV-treated cells, with or without STI571. Colocalization of GFP-HIPK2 and RFP-PML IV was estimated by using the Similarity Feature (Amnis) and quantified (*right panel*). Data represent S.E. from at least three independent experiments.

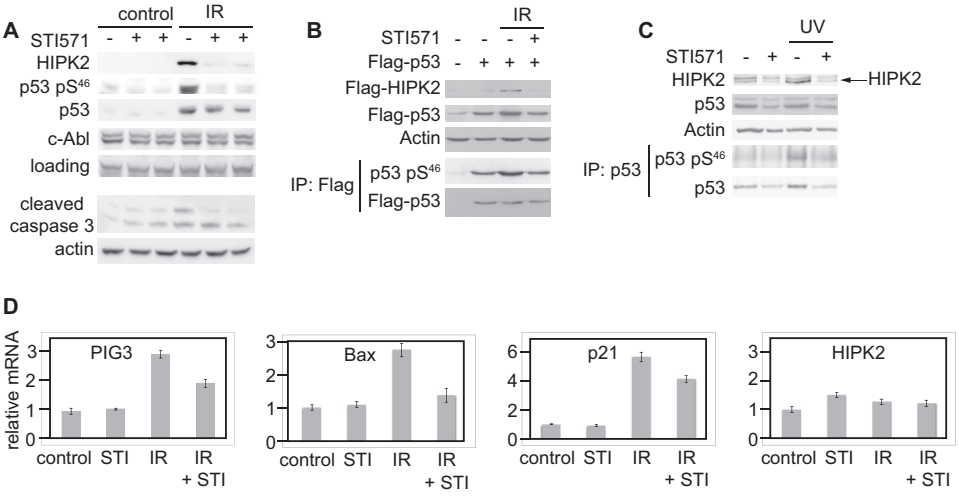

FIGURE 7. **HIPK2 phosphorylation of p53 at Ser46 and apoptotic response to DNA damage is dependent upon c-Abl.** *A*, HepG2 cells were treated with 20 μM STI571 for 2 h and then irradiated (12 Gy) (*IR*). Cells were harvested 24 h (*upper panels*) or 72 h (*lower panels*) later, and cell extracts were analyzed by SDS-PAGE and immunoblotting. Anti-HIPK2 88a was used to detect HIPK2. *pS*^{46}, phospho-Ser^{46}. *B*, Hep3B cells were transfected with pCDNA3 FLAG-HIPK2 (all lanes) and with FLAG-p53, as indicated. Cells were treated with vehicle or 20 μM STI571 24 h after transfection and were irradiated at 12 Gy. Cells were harvested 24 h after IR. FLAG beads were used for IP, and the immunoprecipitates and total samples were analyzed by SDS-PAGE and immunoblotting. *C*, Hep3B cells stably expressing p53 were treated with vehicle or 15 μM STI571 and UV-irradiated at 20 J/m^2, as indicated. Cells were harvested 23 h later, and anti-p53 antibody DO-1 was used to immunoprecipitate and detect p53. Total and immunoprecipitated samples were analyzed by SDS-PAGE and immunoblotting. Anti-HIPK2 C1 was used to detect HIPK2. *D*, HepG2 cells were treated with 20 μM STI571 (*STI*) for 2 h and then irradiated (20 Gy). Cells were harvested 19 h later, and RNA was analyzed by quantitative PCR with the indicated primers, normalized to TBP1. S.E. is calculated from at least three independent experiments.

these data support a model where HIPK2 response to UV and γ-irradiation is dependent upon c-Abl activity. HIPK2 activity is inhibited at high cell density, when c-Abl activation is inhibited by Lats2 (Fig. 8*E*). Environmental conditions, such as cell density, affect cell fate choices in response to DNA damage. Regulation of c-Abl activity by the Hippo pathway enables the cell to modulate its response to DNA damage according to conditions of cell density.

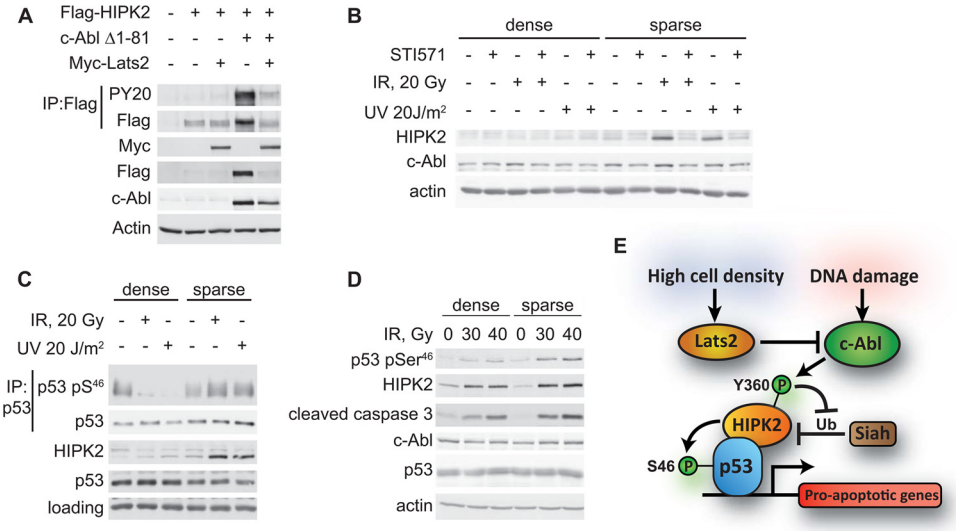

FIGURE 8. **HIPK2 accumulation and activity is inhibited at high cell density.** *A*, Lats2 inhibits c-Abl-induced accumulation of HIPK2. HEK293 cells were transfected with pCDNA3 FLAG-HIPK2, c-Abl Δ1–81, and Myc-Lats2, as indicated. Cells were harvested 24 h following transfection and subjected to IP with α-FLAG-agarose, and immunoprecipitates and total samples were analyzed by SDS-PAGE and immunoblotting. *PY20*, phospho-Tyr. *B–D*, accumulation and activity of HIPK2 due to DNA damage are inhibited at high cell density. *B*, Hep3B cells expressing p53 were plated under sparse and dense conditions. On the following day, they were treated with 15 μM STI571 or vehicle and then γ-irradiated at 20 Gy or UV-irradiated at 20 J/m^2. Cells were harvested 30 h after irradiation and analyzed by SDS-PAGE and immunoblotting. Anti-HIPK2 88a was used to detect HIPK2. *C*, Hep3B cells expressing p53 were treated as in *B*. Cells were harvested 30 h after irradiation, and anti-p53 DO-1 antibody was used to immunoprecipitate and detect p53. Immunoprecipitates and total samples were analyzed by SDS-PAGE and immunoblotting as in *B*. *pS^{46}*, phospho-Ser^{46}. *D*, HEK293 cells were plated under sparse and dense conditions. Cells were γ-irradiated at 30 and 40 Gy, as indicated, and harvested 3 days after IR. Cells were analyzed by SDS-PAGE and immunoblotting as in *B*. *E*, model. c-Abl promotes HIPK2 accumulation and activation of p53. c-Abl is activated by DNA damage and phosphorylates HIPK2. c-Abl inhibits degradation of HIPK2 by Siah-1, and this leads to accumulation of HIPK2. c-Abl may also promote activity of HIPK2 through an unknown mechanism. HIPK2 phosphorylates p53 on Ser^{46}, which promotes apoptosis. At high cell density, c-Abl is inhibited by Lats2, and the above activities are curtailed. Through this mechanism, apoptosis is inhibited in densely plated cells.

Discussion

In this study, we show that the accumulation and activity of HIPK2 in response to DNA damage by IR or UV were dependent on c-Abl kinase activity. Consistently, a reduction in the downstream phosphorylation of p53 at Ser^{46} was also seen upon c-Abl inhibition. Although much is known about response of p53 to DNA damage, many aspects of cell fate decision-making in response to DNA damage are still not well understood. Upon DNA damage, the first objective is to repair the DNA and to restore its proper, lesion-free status. However, with massive DNA damage, perfect repair may not be attainable, and thus the cell must decide from among several cell fates, including apoptosis and senescence. Certain conditions have been shown to promote or prevent particular responses to DNA damage. For example, it is a long-observed phenomenon that cells in culture plated at high cell density are resistant to DNA damage-induced apoptosis. Induction of DNA damage-induced p53-dependent apoptosis is inhibited at high cell density (30). The involvement of high cell density suggested to us that the Hippo pathway, which is activated under these conditions, might play a role in determining cell fate in the DNA damage response. Lats2, a core kinase of the Hippo pathway, inhibits c-Abl, and this prevents Yap/p73-mediated DNA damage-induced apoptosis at high cell density (29). c-Abl had been shown to regulate p53 levels and activity through inhibition of Mdm2 and Mdm4 (24, 38). Here, we show a connection between c-Abl and the p53 apoptotic pathway regulated by HIPK2. Because HIPK2 phosphorylation of p53 at Ser^{46} in response to DNA damage induces apoptotic gene targets (1, 2) as well as the mitochondrial apoptotic program (3, 5), by controlling this activity, the cell can tip the scales toward or against apoptosis. c-Abl is necessary for the apoptotic response mediated by Yap/p73 (20, 21, 27, 39). Because c-Abl promotes both p73 and (through HIPK2) p53 apoptotic activity, regulation of c-Abl activity provides a means of regulating both apoptotic pathways.

HIPK2, like p53, is maintained at low levels in unstressed cells to prevent unwanted apoptosis (16). Several E3 ligases promote the proteasomal degradation of HIPK2, including Siah1/2, WSB1, Mdm2, and SCF(Fbx3) (14, 16–19). Upon DNA damage, degradation of HIPK2 is inhibited through various mechanisms. Association of HIPK2 with PML protects it from degradation mediated by SCF(Fbx3) (14). Our results show that c-Abl was needed for the accumulation of HIPK2 in nuclear speckles and association with PML (Fig. 6). This could represent an additional HIPK2 stabilization mechanism for c-Abl. Siah-1 is phosphorylated by ATM/ATR in response to DNA damage, which inhibits the E3 ligase activity (16). Here, we show that c-Abl phosphorylation of HIPK2 at Tyr^{360} also protects it from Siah-mediated degradation. This double-lock mechanism ensures that HIPK2 will accumulate only under *bona fide* conditions of severe DNA damage.

HIPK2 is also a target of Mdm2 (19). Mdm2 is phosphorylated by c-Abl, and this prevents its ubiquitination of p53 (24). Previous studies have shown a role for c-Abl in preventing Mdm2-mediated degradation of HIPK2 through a different mechanism involving CUL4A activation (40). However, Mdm2 degradation of HIPK2 appears to be more relevant at low, sublethal doses of DNA damage (19). Under our experimental conditions, we have not observed a major role for Mdm2 in HIPK2

degradation or in protection by c-Abl (Ref. 16 and data not shown). However, this does not rule out that under defined conditions, c-Abl also acts through Mdm2 to increase HIPK2 accumulation.

c-Abl was needed for the accumulation of HIPK2 in response to DNA damage, which is mediated, at least in part, by its phosphorylation of HIPK2 at Tyr^{360}. Phosphorylation of Tyr^{360} is not expected, however, to affect HIPK2 kinase activity because mutation of this site does not affect HIPK2 kinase activity (10). Our luciferase reporter assay suggested that c-Abl and HIPK2 synergize to increase p53 activity on the *Bax* and *PIG3* promoters, but the Y360F mutant was not impaired in this assay (Fig. 3). As c-Abl can phosphorylate HIPK2 on additional currently uncharacterized sites (Fig. 1*D*), it is possible that these may play a role in promoting HIPK2 activity. In addition, c-Abl may be acting in an indirect manner, such as by promoting HIPK2 localization to nuclear speckles (Fig. 6), that leads to increased activity through promoting HIPK2 autophosphorylation (12).

Suppression of HIPK2 accumulation at high cell density is consistent with c-Abl inhibition under this condition through the Hippo pathway kinase Lats2 (29). However, we cannot rule out that the Hippo pathway may also be affecting HIPK2 directly. HIPK2 positively regulates the downstream effector of the Hippo pathway, Yki/Yap, in flies and mammals in a kinase-dependent manner (41, 42). This activity is parallel to control of Yki/Yap by Warts/Lats. Whether any feedback loop exists where upstream Hippo pathway components may regulate HIPK2 directly is an interesting avenue to investigate. It will also be interesting to investigate whether c-Abl is involved in HIPK2 activation of Yap under basal conditions, in addition to under DNA damage. Our findings provide evidence for new interplay between Hippo, HIPK2, and the non-receptor tyrosine kinase c-Abl, as well as illustrating network interactions between serine/threonine and tyrosine kinases that dictate cell fate.

Acknowledgments—We thank Moshe Oren and Yael Aylon for helpful discussion and for the reagents, Carol Prives for the anti-p53 antibodies, and Tevie Mehlman for analytical assistance and guidance. STI571 was kindly provided by Novartis Pharmaceuticals.

References

1. Smeenk, L., van Heeringen, S. J., Koeppel, M., Gilbert, B., Janssen-Megens, E., Stunnenberg, H. G., and Lohrum, M. (2011) Role of p53 serine 46 in p53 target gene regulation. *PLoS One* **6,** e17574
2. Feng, L., Hollstein, M., and Xu, Y. (2006) Ser46 phosphorylation regulates p53-dependent apoptosis and replicative senescence. *Cell Cycle* **5,** 2812–2819
3. Mancini, F., Di Conza, G., Pellegrino, M., Rinaldo, C., Prodosmo, A., Giglio, S., D'Agnano, I., Florenzano, F., Felicioni, L., Buttitta, F., Marchetti, A., Sacchi, A., Pontecorvi, A., Soddu, S., and Moretti, F. (2009) MDM4 (MDMX) localizes at the mitochondria and facilitates the p53-mediated intrinsic-apoptotic pathway. *EMBO J.* **28,** 1926–1939
4. Mantovani, F., Tocco, F., Girardini, J., Smith, P., Gasco, M., Lu, X., Crook, T., and Del Sal, G. (2007) The prolyl isomerase Pin1 orchestrates p53 acetylation and dissociation from the apoptosis inhibitor iASPP. *Nat. Struct. Mol. Biol.* **14,** 912–920
5. Sorrentino, G., Mioni, M., Giorgi, C., Ruggeri, N., Pinton, P., Moll, U., Mantovani, F., and Del Sal, G. (2013) The prolyl-isomerase Pin1 activates the mitochondrial death program of p53. *Cell Death Differ.* **20,** 198–208
6. Hofmann, T. G., Möller, A., Sirma, H., Zentgraf, H., Taya, Y., Dröge, W., Will, H., and Schmitz, M. L. (2002) Regulation of p53 activity by its interaction with homeodomain-interacting protein kinase-2. *Nat. Cell Biol.* **4,** 1–10
7. D'Orazi, G., Cecchinelli, B., Bruno, T., Manni, I., Higashimoto, Y., Saito, S., Gostissa, M., Coen, S., Marchetti, A., Del Sal, G., Piaggio, G., Fanciulli, M., Appella, E., and Soddu, S. (2002) Homeodomain-interacting protein kinase-2 phosphorylates p53 at Ser 46 and mediates apoptosis. *Nat. Cell Biol.* **4,** 11–19
8. Puca, R., Nardinocchi, L., Sacchi, A., Rechavi, G., Givol, D., and D'Orazi, G. (2009) HIPK2 modulates p53 activity towards pro-apoptotic transcription. *Mol. Cancer* **8,** 85
9. Dauth, I., Krüger, J., and Hofmann, T. G. (2007) Homeodomain-interacting protein kinase 2 is the ionizing radiation-activated p53 serine 46 kinase and is regulated by ATM. *Cancer Res.* **67,** 2274–2279
10. Saul, V. V., de la Vega, L., Milanovic, M., Krüger, M., Braun, T., Fritz-Wolf, K., Becker, K., and Schmitz, M. L. (2013) HIPK2 kinase activity depends on cis-autophosphorylation of its activation loop. *J. Mol. Cell Biol.* **5,** 27–38
11. Siepi, F., Gatti, V., Camerini, S., Crescenzi, M., and Soddu, S. (2013) HIPK2 catalytic activity and subcellular localization are regulated by activation-loop Y354 autophosphorylation. *Biochim. Biophys. Acta* **1833,** 1443–1453
12. Bitomsky, N., Conrad, E., Moritz, C., Polonio-Vallon, T., Sombroek, D., Schultheiss, K., Glas, C., Greiner, V., Herbel, C., Mantovani, F., del Sal, G., Peri, F., and Hofmann, T. G. (2013) Autophosphorylation and Pin1 binding coordinate DNA damage-induced HIPK2 activation and cell death. *Proc. Natl. Acad. Sci. U.S.A.* **110,** E4203–E4212
13. Möller, A., Sirma, H., Hofmann, T. G., Rueffer, S., Klimczak, E., Dröge, W., Will, H., and Schmitz, M. L. (2003) PML is required for homeodomain-interacting protein kinase 2 (HIPK2)-mediated p53 phosphorylation and cell cycle arrest but is dispensable for the formation of HIPK domains. *Cancer Res.* **63,** 4310–4314
14. Shima, Y., Shima, T., Chiba, T., Irimura, T., Pandolfi, P. P., and Kitabayashi, I. (2008) PML activates transcription by protecting HIPK2 and p300 from SCF^{Fbx3}-mediated degradation. *Mol. Cell. Biol.* **28,** 7126–7138
15. Polonio-Vallon, T., Kirkpatrick, J., Krijgsveld, J., and Hofmann, T. G. (2014) Src kinase modulates the apoptotic p53 pathway by altering HIPK2 localization. *Cell Cycle* **13,** 115–125
16. Winter, M., Sombroek, D., Dauth, I., Moehlenbrink, J., Scheuermann, K., Crone, J., and Hofmann, T. G. (2008) Control of HIPK2 stability by ubiquitin ligase Siah-1 and checkpoint kinases ATM and ATR. *Nat. Cell Biol.* **10,** 812–824
17. Calzado, M. A., de la Vega, L., Möller, A., Bowtell, D. D., and Schmitz, M. L. (2009) An inducible autoregulatory loop between HIPK2 and Siah2 at the apex of the hypoxic response. *Nat. Cell Biol.* **11,** 85–91
18. Choi, D. W., Seo, Y. M., Kim, E. A., Sung, K. S., Ahn, J. W., Park, S. J., Lee, S. R., and Choi, C. Y. (2008) Ubiquitination and degradation of homeodomain-interacting protein kinase 2 by WD40 repeat/SOCS box protein WSB-1. *J. Biol. Chem.* **283,** 4682–4689
19. Rinaldo, C., Prodosmo, A., Mancini, F., Iacovelli, S., Sacchi, A., Moretti, F., and Soddu, S. (2007) MDM2-regulated degradation of HIPK2 prevents p53Ser46 phosphorylation and DNA damage-induced apoptosis. *Mol. Cell* **25,** 739–750
20. Agami, R., Blandino, G., Oren, M., and Shaul, Y. (1999) Interaction of c-Abl and p73α and their collaboration to induce apoptosis. *Nature* **399,** 809–813
21. Levy, D., Adamovich, Y., Reuven, N., and Shaul, Y. (2008) Yap1 phosphorylation by c-Abl is a critical step in selective activation of proapoptotic genes in response to DNA damage. *Mol. Cell* **29,** 350–361
22. Levy, D., Reuven, N., and Shaul, Y. (2008) A regulatory circuit controlling Itch-mediated p73 degradation by Runx. *J. Biol. Chem.* **283,** 27462–27468
23. Cottini, F., Hideshima, T., Xu, C., Sattler, M., Dori, M., Agnelli, L., ten Hacken, E., Bertilaccio, M. T., Antonini, E., Neri, A., Ponzoni, M., Marcatti, M., Richardson, P. G., Carrasco, R., Kimmelman, A. C., Wong, K. K., Caligaris-Cappio, F., Blandino, G., Kuehl, W. M., Anderson, K. C., and Tonon, G. (2014) Rescue of Hippo coactivator YAP1 triggers DNA damage-induced apoptosis in hematological cancers. *Nat. Med.* **20,** 599–606
24. Goldberg, Z., Vogt Sionov, R., Berger, M., Zwang, Y., Perets, R., Van Etten, R. A., Oren, M., Taya, Y., and Haupt, Y. (2002) Tyrosine phosphorylation

of Mdm2 by c-Abl: implications for p53 regulation. *EMBO J.* **21,** 3715–3727
25. Kharbanda, S., Yuan, Z. M., Weichselbaum, R., and Kufe, D. (1998) Determination of cell fate by c-Abl activation in the response to DNA damage. *Oncogene* **17,** 3309–3318
26. Wang, X., Zeng, L., Wang, J., Chau, J. F., Lai, K. P., Jia, D., Poonepalli, A., Hande, M. P., Liu, H., He, G., He, L., and Li, B. (2011) A positive role for c-Abl in Atm and Atr activation in DNA damage response. *Cell Death Differ.* **18,** 5–15
27. Yuan, Z. M., Shioya, H., Ishiko, T., Sun, X., Gu, J., Huang, Y. Y., Lu, H., Kharbanda, S., Weichselbaum, R., and Kufe, D. (1999) p73 is regulated by tyrosine kinase c-Abl in the apoptotic response to DNA damage. *Nature* **399,** 814–817
28. Ben-Yehoyada, M., Ben-Dor, I., and Shaul, Y. (2003) c-Abl tyrosine kinase selectively regulates p73 nuclear matrix association. *J. Biol. Chem.* **278,** 34475–34482
29. Reuven, N., Adler, J., Meltser, V., and Shaul, Y. (2013) The Hippo pathway kinase Lats2 prevents DNA damage-induced apoptosis through inhibition of the tyrosine kinase c-Abl. *Cell Death Differ.* **20,** 1330–1340
30. Bar, J., Cohen-Noyman, E., Geiger, B., and Oren, M. (2004) Attenuation of the p53 response to DNA damage by high cell density. *Oncogene* **23,** 2128–2137
31. Weidtkamp-Peters, S., Lenser, T., Negorev, D., Gerstner, N., Hofmann, T. G., Schwanitz, G., Hoischen, C., Maul, G., Dittrich, P., and Hemmerich, P. (2008) Dynamics of component exchange at PML nuclear bodies. *J. Cell Sci.* **121,** 2731–2743
32. Hobbs, S., Jitrapakdee, S., and Wallace, J. C. (1998) Development of a bicistronic vector driven by the human polypeptide chain elongation factor 1α promoter for creation of stable mammalian cell lines that express very high levels of recombinant proteins. *Biochem. Biophys. Res. Commun.* **252,** 368–372
33. Haupt, Y., Maya, R., Kazaz, A., and Oren, M. (1997) Mdm2 promotes the rapid degradation of p53. *Nature* **387,** 296–299
34. Okada, N., Yabuta, N., Suzuki, H., Aylon, Y., Oren, M., and Nojima, H. (2011) A novel Chk1/2-Lats2-14-3-3 signaling pathway regulates P-body formation in response to UV damage. *J. Cell Sci.* **124,** 57–67
35. Levy, D., Adamovich, Y., Reuven, N., and Shaul, Y. (2007) The Yes-associated protein 1 stabilizes p73 by preventing Itch-mediated ubiquitination of p73. *Cell Death Differ.* **14,** 743–751
36. Ortyn, W. E., Perry, D. J., Venkatachalam, V., Liang, L., Hall, B. E., Frost, K., and Basiji, D. A. (2007) Extended depth of field imaging for high speed cell analysis. *Cytometry A* **71,** 215–231
37. Buchdunger, E., Cioffi, C. L., Law, N., Stover, D., Ohno-Jones, S., Druker, B. J., and Lydon, N. B. (2000) Abl protein-tyrosine kinase inhibitor STI571 inhibits in vitro signal transduction mediated by c-Kit and platelet-derived growth factor receptors. *J. Pharmacol. Exp. Ther.* **295,** 139–145
38. Zuckerman, V., Lenos, K., Popowicz, G. M., Silberman, I., Grossman, T., Marine, J. C., Holak, T. A., Jochemsen, A. G., and Haupt, Y. (2009) c-Abl phosphorylates Hdmx and regulates its interaction with p53. *J. Biol. Chem.* **284,** 4031–4039
39. Gong, J. G., Costanzo, A., Yang, H. Q., Melino, G., Kaelin, W. G., Jr., Levrero, M., and Wang, J. Y. (1999) The tyrosine kinase c-Abl regulates p73 in apoptotic response to cisplatin-induced DNA damage. *Nature* **399,** 806–809
40. Raina, D., Ahmad, R., Chen, D., Kumar, S., Kharbanda, S., and Kufe, D. (2008) MUC1 oncoprotein suppresses activation of the ARF-MDM2-p53 pathway. *Cancer Biol. Ther.* **7,** 1959–1967
41. Chen, J., and Verheyen, E. M. (2012) Homeodomain-interacting protein kinase regulates Yorkie activity to promote tissue growth. *Curr. Biol.* **22,** 1582–1586
42. Poon, C. L., Zhang, X., Lin, J. I., Manning, S. A., and Harvey, K. F. (2012) Homeodomain-interacting protein kinase regulates Hippo pathway-dependent tissue growth. *Curr. Biol.* **22,** 1587–1594